Joint Optimization of Transmission Power Level and Packet Size for WSN Lifetime Maximization

Ayhan Akbas, Huseyin Ugur Yildiz, Bulent Tavli, and Suleyman Uludag

***Abstract*—In pursuit of better energy efficiency and enhanced network lifetime in Wireless Sensor Networks (WSNs), two crucial factors are data packet size and transmission power level. On one hand, smaller packet size reduces the overall impact of bit error rates on packet loss. However, the consequence of smaller packet size is fragmentation into more data packets and thereby dissipation of increased energy. Hence, there emerges a delicate engineering tradeoff in deciding the data packet size where both low and high data packet size decisions lead to certain energy inefficiency issues. On the other hand, increasing transmission power level decreases packet loss probability, which is another decision variable to optimize for maximizing network lifetime. Joint consideration of these two factors exacerbates the complexity of the optimization problem for the objective of the network lifetime maximization. In this study, we develop a realistic WSN link layer model built on top of the empirically verified energy dissipation characteristics of Mica2 motes and WSN channel models. We make use of the aforementioned link layer model to design a novel Mixed Integer Programming (MIP) framework for joint optimization of transmission power level and data packet size to take up the challenge introduced above. Numerical evaluations of the MIP framework with analysis of the results over a large parameter space are performed to characterize the effects of joint optimization of packet size and power level on WSN lifetime.**

***Index Terms*—wireless sensor networks, network lifetime, mixed integer programming, transmission power control, data packet size, energy efficiency.**

I. Introduction

Constructed from resource-constrained computing devices or sensors, Wireless Sensor Networks (WSNs) have become remarkably effective in a variety of application areas [1]–[3]. A unifying characteristic is the task of data collection through sensing, measuring, and communicating. However, WSNs suffer from the shortage of operational lifetime which is defined as the period between the deployment and the time that the first node dies [4]. Therefore it is crucial that all nodes of WSNs dissipate their energy in a balanced fashion so that early battery exhaustion of any node is delayed to the extent possible [5].

Researchers focus on the power management policies in order to maximize the functional network lifetime by reducing unnecessary power consumption and by using the available energy effectively. To accomplish the goal of WSN lifetime maximization, it becomes evident that transmission energy dissipation must be intelligently managed as the most dominant term in overall energy consumption comes from communication.

Data packet size is another equally important energy efficiency parameter in efforts to improve WSN network lifetime. The use of a smaller packet size reduces the overall impact of bit error rates on packet loss. However, a smaller packet size results in more packets to be transmitted under the most likely fixed protocol header scenarios. Thus, for a given amount of data, employment of a smaller packet size will inflate the number of bits to transmit, resulting in dissipation of more energy than otherwise. Hence, there emerges a delicate engineering tradeoff in deciding the data packet size where both low and high values lead to certain energy inefficiency issues.

While studying the impact of data packet size and transmission power levels individually is challenging, the complexity is exacerbated when they are considered simultaneously. In this paper, our goal is to characterize the joint impact of the packet size and the transmission power levels in WSN with respect to the network lifetime objective. Our contributions are as follows:

1) A novel network lifetime optimization formulation for WSNs is developed via a mixed integer programming (MIP) framework by means of the joint consideration of packet size and transmission power levels,
2) A link layer model that abstracts the WSN characteristics based on the empirically verified energy dissipation characteristics of Mica2 motes in conjunction with an empirically verified channel model is constructed which can be utilized with minor modifications to investigate many other WSN problems,

The remainder of the paper is organized as follows: Related work is given in Section II. Section III presents the system model, link layer model, and the MIP framework. In Section IV, performance evaluation of the developed approach is given. Section V provides our concluding remarks and discussions of the results.

II. Related Work

The literature on the packet size optimization is quite rich for various channel models. Majority are for free space [6]–[9], some for underwater [10], [11], terrestrial and underground [12]. There are some application specific studies for body area [13], [14] and smart meter networking [15]. Our study diverges from these studies in several aspects. In [8], [9], [11], [12], [14], [16]–[18], authors utilize Automatic Repeat Request (ARQ) schemes that assume lossless perfect feedback

A. Akbas, H.U. Yildiz, and B. Tavli are with TOBB University of Economics and Technology, 06520, Ankara, Turkey (e-mail: {aakbas, huyildiz, btavli}@etu.edu.tr).

S. Uludag is with the University of Michigan - Flint, Flint, MI, 48502, USA (e-mail: uludag@umich.edu).

channel in general. In [6], [19], authors utilize proprietary schemes RTS (Request-To-Send)-CTS (Clear-To-Send)-ACK (Acknowledgement) packet sequence and AggACK, respectively. Proposed approaches are prone to bit errors. Our study implements a complete link-layer handshaking cycle and acknowledgement feedback which has been verified with real-world data. Contrary to the studies using Additive White Gaussian Noise (AWGN) and Rayleigh fading channel model [7], [12], [14], [17], [20]–[22], we employ a log-normal shadowing path loss communication channel model as in [8], [9] due to the empirically verified energy dissipation characteristics of Mica2 motes.

In [15], [18], [21]–[23], authors have taken transmit power level into account or assumed to have a constant fix term. [7] used higher power to overcome Signal-to-Noise ratio (SNR). [16] assumes that transceiver adjusts its transmit power so as to achieve a given level of received power at its intended receiver. [8] and [9] use fix and adaptive power schemes to investigate a sustainable communications channel with tolerable BER and to have the highest energy efficiency for detection probability. [6] argues that transmission power is an effective parameter on packet size at different distances and transmission powers, stating that the optimal packet size varies in different conditions.

Our goal of the maximization of the network lifetime also differs from the literature whose goal is mainly to optimize or maximize the energy efficiency of WSNs [11], [13], [14], [18], [21]–[24] or resource utilization [12]. Their primary target to have optimal packet size is a better channel utilization or performance via optimization of channel parameters [6], [7], a sustainable communication under tolerable BER [8], a better QoS channel quality [25], a higher detection probability [9] or the optimization of cross technology interference [20].

To the best of our knowledge, there is no published work that has targeted a maximized network lifetime of WSNs, especially jointly with the transmit power level control and packet size [1]. A close study presented in [8] aims a sustainable communication channel, focusing on shadowing effects rather than maximum network lifetime and uses different assumptions and infinite ARQ scheme in contrary to our complete link-layer handshaking cycle with ACK feedback.

III. System Model

In this paper, we assume that a data packet is comprised of a header and a payload. Header part contains information such as current segment number, total number of segments, event/location/attribute identifiers, *etc*. Payload field contains the information bits. To maximize the network lifetime, the payload-size/packet-size ratio has to be maximized since the header part cannot be avoided and of fixed size. If perfect channel conditions are present (*i.e.*, no packet errors) the best result can be obtained by using the largest possible payload data packed into a single packet, so that the highest data carrying capacity is achieved. However, as the packet size increases, the probability of re-transmissions also goes up. On the other hand, smaller packets would have a higher successful transmission rate, but this will lead to: (i) more power to dissipate due to the small payload-size/packet-size ratio, (ii) transmission latency and difficult packet management due to higher number of packets, and (iii) additional decoding/encoding overhead.

[1]A preliminary version of this work is presented in [26].

A. Overview

We consider a WSN consisting of a stationary single base station and multiple stationary sensor nodes, where N_S denotes the number of sensor nodes. Nodes are deployed over a sensing area to collect data from the environment, as shown in Fig. 1.

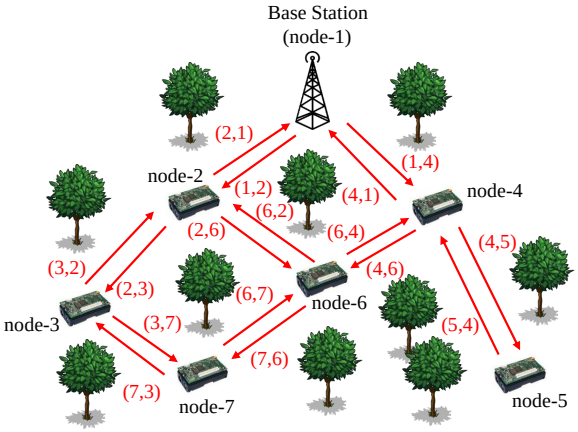

Fig. 1: A typical WSN architecture.

Table I provides the notations we use in our formulations. WSN topology is represented as a directed graph, $G(V, A)$, where V denotes the set of all nodes including the base station as node-1. We also define the set W that includes all nodes except the base station node-1 (*i.e.*, $W = V \setminus \{1\}$). $A = \{(i, j) : i \in W, j \in \{V - i\}\}$ is the ordered set of arcs. Note that, the definition of A implies that no node sends data to itself. The number of data packets flowing from node-i to node-j is denoted by f_{ij}.

We assume that the path loss for each link is measured by a closed loop power control mechanism. The energy costs of topology discovery and route creation operations constitute a small fraction of the total network energy dissipation. We assume that all nodes are time synchronized[2]. Nodes transmit collected data to the base station either directly (single-hop) or act as a relay for other nodes (multi-hop). In addition, we assume that a TDMA-based MAC layer is in operation to mitigate interference between active links through a time-slot assignment algorithm. Time is organized into *rounds* where each round lasts 60 seconds (*i.e.*, $T_{rnd} = 60$ s). At each round, s_i number of packets are generated and relayed to the base station. Generated data packets at sensor nodes are treated as

[2]There are many synchronization protocols designed specifically for WSNs with virtually no overhead and satisfactory synchronization performance [27]. For example, timing-sync protocol uses piggybacking for synchronization [28], which is reported to have an average synchronization error of 16.9 μs and a worst case error of 44 μs. We assume such a low overhead time synchronization protocol is used in the network.

TABLE I: Nomenclature used in our formulations.

Sy/Ac/Vr	Description	Sy/Ac/Vr	Description
N_{rnd}	Number of rounds	T_{rnd}	Duration of a round (60 s)
f_{ij}	Number of data packets flowing from node-i to node-j	ϱ	Initial energy assigned to sensor nodes (25 KJ)
s_i	Number of data packets generated at node-i at each round	N_S	Number of nodes
d_{ij}	Distance between node-i and node-j	E_{PP}	Packet processing energy (120 μJ)
$P_{tx}^{crc}(l)$	Power consumption for transmission at power level-l	$P_{tx}^{ant}(l)$	Output antenna power at power level-l
P_{rx}^{crc}	Power consumption for reception (35.4 mW)	ξ	Channel data rate (19.2 kbps)
E_{DA}	Data acquisition energy (600 μJ)	T_{DA}	Data processing time (20 ms)
M_P	Payload Size (30–240 Bytes)	M_H	Header Size (16 Bytes)
M_D	Data packet size (46–256 Bytes)	M_A	ACK packet size (20 Bytes)
T_{slot}	Slot time	T_{grd}	Guard time (100 μs)
T_{rsp}	Response time (500 μs)	P_{slp}	Power consumption in the sleep mode (3 μW)
$T_{tx}(\varphi)$	Duration of a φ-Byte packet transmission	n	path loss exponent (3.69)
Υ_{ij}	Path loss at a distance d_{ij} (dB)	Υ_0	Path loss at the reference distance (31 dB)
X_σ	Zero-mean Gaussian random variable with standard deviation $\sigma = 1.42$ that represents shadowing (dB)	P_n	Noise Floor (-115 dBm)
$\psi_{ij}(l)$	SNR at node-j due to the transmission of node-i at power level-l (dB)	$P_{rx,ij}^{ant}(l)$	The received signal power due to a transmission at power level-l over the link-(i,j) (dB)
$p_{ij}^{s}(l,\varphi)$	Probability of successful packet reception for a φ-Byte packet transmitted at power level-l over the link-(i,j)	$p_{ij}^{f}(l,\varphi)$	Probability of failed packet reception for a φ-Byte packet transmitted at power level-l over the link-(i,j)
$p_{ij}^{HS,s}(l,k)$	Probability of a successful handshake	$p_{ij}^{HS,f}(l,k)$	Probability of a failed handshake
$\lambda_{ij}(l,k)$	Packet retransmission rate for the link-(i,j)	P_{sns}	Sensitivity level (-102 dBm)
$E_{tx}^{P}(l,\varphi)$	Energy for transmitting an M_D-Byte packet data at power level-l	$E_{tx}^{HS}(l,M_D)$	Total energy dissipation of a transmitter in a slot
$E_{tx,ij}^{D}(l,k)$	Energy consumption of a transmitter for completing a handshake including retransmissions	$E_{rx,ji}^{D}(l,k)$	Energy consumption of a receiver for completing a handshake including retransmissions
$E_{rx}^{HS,s}(k,M_A)$	Energy dissipation of a receiver for a successful handshake	$E_{rx}^{HS,f}$	Energy dissipation of a receiver for a failed handshake due to data packet errors
$T_{bsy,i}$	Total busy time of node-i	I_{jn}^{i}	Interference function
l_{min}	Minimum power level (level-1)	l_{max}	Maximum power level (level-26)
l_{ij}^{opt}	Optimum power level to transmit a data packet from node-i to node-j	k_{ji}^{opt}	Optimum power level to transmit an ACK packet from node-j to node-i
S_L	Set of all power levels	$G(V,A)$	Directed graph that represents network topology
V	Set of nodes, including the base station as node-1	W	Set of sensor nodes

atomic data units that cannot be fragmented or aggregated at any relay node.

A successful handshake is performed if both data and ACK packets are received without errors by the intended recipients. There are two possible cases for unsuccessful handshake. First, the data packet can be received without any errors but the ACK packet may fail. Second, the data packet may not be received error-free and thus no ACK packets are sent to the transmitter. In such cases, the handshake must be repeated which leads to extra energy dissipation.

B. Data Link Layer Model

We utilize Mica2 motes' [29] energy consumption characteristics equipped with CC1000 radios which are the most commonly utilized sensor nodes in experimental WSN research due to their well-characterized energy dissipation properties [30], [31]. In Table II, power consumption of the transceiver and the corresponding output antenna power are presented. In this table, $P_{tx}^{crc}(l)$ and $P_{tx}^{ant}(l)$ refer to the power consumption for transmission at power level-l, and the output antenna power at power level-l, respectively. The set of power levels is denoted by S_L. Power consumption for reception is assumed to be constant at 35.4 mW (*i.e.*, $P_{rx}^{crc} = 35.4$ mW). Packet headers include a two Byte CRC (Cyclic Redundancy Check) for checking data integrity against possible bit errors. The CRC computation is a running calculation which does not require a separate pass on the received data packet. Hence, energy dissipation for CRC check is accounted for in P_{rx}^{crc}.

At each round, energy dissipation for data acquisition is $E_{DA} = 600$ μJ and each node produces the same amount of raw data as 240 Bytes. In our framework, the size of the data payload packet is denoted by M_P which varies between 30 Bytes and 240 Bytes, which are dividers of 240 (*i.e.*, 240, 120, 80, 60, 48, 40, and 30 Bytes). Hence we utilize 7 possible

TABLE II: Transmission power consumption ($P_{tx}^{crc}(l)$ in mW) and output antenna power ($P_{tx}^{ant}(l)$ in mW) at each power level (l) for the Mica2 motes equipped with CC1000 for different power levels (l) [30].

l	$P_{tx}^{crc}(l)$	$P_{tx}^{ant}(l)$	l	$P_{tx}^{crc}(l)$	$P_{tx}^{ant}(l)$
1 (l_{min})	25.8	0.0100	14	32.4	0.1995
2	26.4	0.0126	15	33.3	0.2512
3	27.0	0.0158	16	41.4	0.3162
4	27.1	0.0200	17	43.5	0.3981
5	27.3	0.0251	18	43.6	0.5012
6	27.8	0.0316	19	45.3	0.6310
7	27.9	0.0398	20	47.4	0.7943
8	28.5	0.0501	21	50.4	1.0000
9	29.1	0.0631	22	51.6	1.2589
10	29.7	0.0794	23	55.5	1.5849
11	30.3	0.1000	24	57.6	1.9953
12	31.2	0.1259	25	63.9	2.5119
13	31.8	0.1585	26 (l_{max})	76.2	3.1623

payload sizes. Each node can adjust the number of data packets to be transmitted at each round according to the given payload sizes. For example, if a node utilizes 240 Bytes of payload, then it would transmit 1 data packet at each round. However, if this node utilizes 120 Bytes of payload, then it would transmit 2 data packets at each round. Same procedure applies for the rest of the payload sizes. As stated before, we denote s_i to represent the number of data packets to be transmitted at each round by node-i. The size of a data packet including a 16 Byte header ($M_H = 16$ Bytes) varies between 46 Bytes and 256 Bytes (*i.e.*, $M_D = M_P + M_H$).

The size of an ACK packet is $M_A = 20$ Bytes. Guard time is set to $T_{grd} = 100$ μs, which is roughly twice the maximum synchronization error [27], [28]. The time interval between the completion of the data packet transmission at the source node and the beginning of the ACK packet receipt which includes various delay terms, such as propagation delay, is modeled by $T_{rsp} = 500$ μs. Hence, the slot time, T_{slot}, is calculated as $T_{slot} = [2 \times T_{grd} + T_{tx}(M_D) + T_{rsp} + T_{tx}(M_A)]$ where $T_{tx}(M_D)$ and $T_{tx}(M_A)$ are the durations of data and ACK packets, respectively, and are obtained by dividing the number of bits to the channel data rate ($\xi = 19.2$ Kbps) [29].

The received signal power ($P_{rx,ij}^{ant}(l)$) due to a transmission at power level-l over the link-(i,j) is

$$P_{rx,ij}^{ant}(l)[\text{dBm}] = P_{tx}^{ant}(l)[\text{dBm}] - \Upsilon_{ij}[\text{dB}], \tag{1}$$

where Υ_{ij} denotes the path loss value over link (i,j). The log-normal shadowing path loss model can, mathematically, be expressed as

$$\Upsilon_{ij}[\text{dB}] = \Upsilon_0[\text{dB}] + 10n\log_{10}(d_{ij}/d_0) + X_\sigma \ \ [\text{dB}], \tag{2}$$

where d_{ij} is the distance between transmitter and receiver, d_0 is the reference distance, Υ_0 is the path loss at the reference distance, n is the path loss exponent (*i.e.*, the rate at which the signal decays). X_σ is a zero-mean Gaussian random variable with the standard deviation σ dB to model large-scale fading (shadowing) effects.

We adopt the parameter values provided for Mica2 motes as n = 3.69, σ = 1.42 dB, d_0 = 1 m, and Υ_0 = 31 dB [32].

SNR is defined as

$$\psi_{ij}(l)[\text{dB}] = P_{rx,ij}^{ant}(l)[\text{dBm}] - P_n[\text{dBm}], \tag{3}$$

where the noise power (P_n) is – 115 dBm at the temperature of 300 Kelvin for Mica2 motes [33].

For non-coherent frequency shift keying (FSK) modulation scheme, as used in used in Mica2 motes, the probability of a successful packet reception of a φ-Byte packet transmitted at power level-l over the link-(i,j) [33] is

$$p_{ij}^{s}(l,\varphi) = \left(1 - \frac{1}{2}\exp\left(\frac{-\psi_{ij}(l)}{2}\frac{1}{0.64}\right)\right)^{8\varphi}, \tag{4}$$

and the failure probability is calculated as

$$p_{ij}^{f}(l,\varphi) = 1 - p_{ij}^{s}(l,\varphi). \tag{5}$$

The probability of a successful handshake when the data packet is transmitted at power level-l and acknowledged at power level-k over the link-(i,j) is

$$p_{ij}^{HS,s}(l,k) = p_{ij}^{s}(l,M_D) \times p_{ji}^{s}(k,M_A), \tag{6}$$

provided that $P_{rx,ij}^{ant}(l) \geq P_{sns}$ and $P_{rx,ji}^{ant}(k) \geq P_{sns}$. Otherwise (*i.e.*, $P_{rx,ij}^{ant}(l) < P_{sns}$ or $P_{rx,ji}^{ant}(k) < P_{sns}$), $p_{ij}^{HS,s}(l,k) = 0$ where P_{sns} denotes the reception sensitivity of the Mica2 motes (P_{sns} = – 102 dBm) [30]. We call this condition as the *sensitivity criterion*. The probability of a failed handshake is given as

$$p_{ij}^{HS,f}(l,k) = 1 - p_{ij}^{HS,s}(l,k). \tag{7}$$

On the average, each data packet has to be transmitted $\lambda_{ij}(l,k) = 1/p_{ij}^{HS,s}(l,k)$ times. Energy dissipation for transmitting M_D Bytes of data from node-i to node-j at power level-l is,

$$E_{tx}^{P}(l,M_D) = P_{tx}^{crc}(l)T_{tx}(M_D). \tag{8}$$

A node stays in receiving mode when it is not transmitting. Hence, the total energy dissipation of a transmitter in a slot during a single handshake is

$$E_{tx}^{HS}(l,M_D) = E_{tx}^{P}(l,M_D) + P_{rx}^{crc}(T_{slot} - T_{tx}(M_D)). \tag{9}$$

Transmitter's energy dissipation including packet failures and processing cost is

$$E_{tx,ij}^{D}(l,k) = E_{PP} + \lambda_{ij}(l,k)E_{tx}^{HS}(l,M_D), \tag{10}$$

where $E_{PP} = 120$ μJ.

Energy dissipation for receiving a data packet and replying with an ACK packet without any packet error (*i.e.* a successful handshake) is

$$E_{rx}^{HS,s}(k,M_A) = P_{rx}^{crc}(T_{slot} - T_{tx}(M_A)) + E_{tx}^{P}(k,M_A). \tag{11}$$

If the handshake failure is caused by bit errors in the received data packet, then the energy cost for reception can be expressed as

$$E_{rx}^{HS,f} = P_{rx}^{crc}T_{slot}. \tag{12}$$

Receiver's energy dissipation including the effects of packet failures can be obtained as

$$E_{rx,ji}^{D}(l,k) = E_{rx}^{HS,s}(k,M_A) + E_{PP} + \lambda_{ij}(l,k) \times \left[p_{ij}^{s}(l,M_D)p_{ji}^{f}(k,M_A)E_{rx}^{HS,s}(k,M_A) + p_{ij}^{f}(l,M_D)E_{rx}^{HS,f}\right] \tag{13}$$

C. MIP Framework

In this subsection, we present the MIP framework used to jointly optimize the transmission power and packet size for the objective of WSN lifetime maximization. The optimization problem is presented in Fig. 2. Note that, unitless variable N_{rnd} gives the network lifetime in terms of the number of rounds and the actual network lifetime can be expressed by the product $N_{rnd} \times T_{rnd}$.

Flow balancing constraint at each sensor node (*i.e.*, $\forall i \in W$) is given in (16). It states that data flowing into node-i plus data generated by node-i is equal to the data flowing out of node-i.

Energy balancing constraint is given in (17) which states that, for all nodes except the base station, the total energy dissipation is bounded from above by the energy stored in batteries (ϱ). Energy dissipation terms on the left hand side of the inequality in (17) accounts for transmission, sleep, reception, and data acquisition energies, respectively. Note that, if a node is neither a receiver nor a transmitter at any time slot or if it is not acquiring data then it is in the *sleep* mode. Hence, the total sleep time can be obtained from the total busy time which is calculated as $N_{rnd}T_{rnd} - T_{bsy,i}$. In this equation, $T_{bsy,i}$ is defined as the total amount of time that node-i stays busy and it is calculated as

$$T_{bsy,i} = T_{slot}\left[\sum_{(i,j)\in A}\lambda_{ij}(l,k)f_{ij} + \sum_{(j,i)\in A}\lambda_{ji}(l,k)f_{ji}\right] + N_{rnd}T_{DA}, \quad \forall i \in W. \tag{14}$$

Power consumption in sleep mode is taken as 3 μW (*i.e.*, $P_{slp} = 3$ μW). Each sensor node is provided with equal initial energy ($\varrho = 25$ KJ) at the beginning of the network operation.

The *bandwidth constraint* is presented in (18). In this equation, it is guaranteed that the channel bandwidth required to perform communication operations at each node is strictly bounded by the available bandwidth. For all nodes including the base station, the aggregate duration of incoming flows, outgoing flows, and interfering flows is upper bounded by the total network lifetime. This constraint is a modified version of the sufficient condition given in [31].

We refer to the flows around node-i which are not flowing into or flowing out of node-i, however, affect the available bandwidth of node-i as *interfering flows*. Interference function ($I^i_{jn}(l,k)$) is formulated in (19). If node-i is in the interference region of the transmission from node-j to node-n at power level-l (data transmission) or node-n to node-j at power level-k (ACK transmission), then the value of interference function for node-i is unity ($i \neq j \neq n$), otherwise it is zero. Finally, (20) states that all flows are non-negative, the *non-negativity constraint*.

The MIP model presented in Fig. 2 assumes that the data and ACK transmission power levels are determined for each link by considering the energy dissipations as given in (10) and (13) on each link individually and separately. Therefore, we determine a single optimal power level for data packet transmission (l^{opt}_{ij}) and a single optimal power level for ACK packet transmission (k^{opt}_{ji}) for each link-(i,j). That is, on link-(i,j) data packets are transmitted at power level-l^{opt}_{ij} by node-i and ACK packets are transmitted at power level-k^{opt}_{ji} by node-j. The optimal power levels are determined by using the following link scope optimization scheme (*i.e.*, transmission power level optimization is performed on each link locally)

$$\{l^{opt}_{ij}, k^{opt}_{ji}\} = \underset{l\in S_L k\in S_L}{\operatorname{argmin}}\left(E^D_{tx,ij}(l,k) + E^D_{rx,ji}(l,k)\right). \tag{15}$$

Optimal flows on each link (f_{ij}) are determined by using the predetermined data/ACK transmission power levels and retransmission rates for each link, however, determination of the flows is a global optimization process. Nevertheless, we do not have a direct constraint in the MIP model that rules out the use of a link which has a lower bit error rate than a predetermined value. However, if it is possible to route the data flows by using lower energy dissipating links which have low bit error rates then the optimization process decides to use those links and avoids the higher bit rate links. When the sensitivity criterion is active, links that have high path loss values which do not allow the received power level to be higher than the sensitivity threshold (even if the highest transmission power level is utilized) are not allowed to be used in the solution of the MIP problem (*i.e.*, those links are removed from the network topology).

Maximize N_{rnd}
Subject to:

$$\sum_{(i,j)\in A} f_{ij} - \sum_{(j,i)\in A} f_{ji} = N_{rnd}s_i \ \forall i \in W \tag{16}$$

$$\underbrace{\sum_{(i,j)\in A} E^D_{tx,ij}(l,k)f_{ij}}_{\textbf{transmission}} + \underbrace{P_{slp}(N_{rnd}T_{rnd} - T_{bsy,i})}_{\textbf{sleep}} + \underbrace{\sum_{(j,i)\in A} E^D_{rx,ji}(l,k)f_{ji}}_{\textbf{reception}} + \underbrace{N_{rnd}E_{DA}}_{\textbf{acquisiton}} \leq \varrho \ \forall i \in W \tag{17}$$

$$T_{slot}\left[\sum_{(i,j)\in A}\lambda_{ij}(l,k)f_{ij} + \sum_{(j,i)\in A}\lambda_{ji}(l,k)f_{ji} + \sum_{(j,n)\in A}\lambda_{jn}(l,k)f_{jn}I^i_{jn}(l,k)\right] \leq N_{rnd}T_{rnd}, \ \forall i \in V \tag{18}$$

$$I^i_{jn}(l,k) = \begin{cases} 1 \text{ if } P^{ant}_{rx,ji}(l) \geq P_{sns} \text{ or} \\ \quad P^{ant}_{rx,ni}(k) \geq P_{sns} \\ 0 \text{ o.w.} \end{cases} \tag{19}$$

$$f_{ij} \geq 0 \ \forall (i,j) \in A \tag{20}$$

Fig. 2: MIP framework.

IV. Numerical Analysis

In this section, we present the results of numerical analysis to investigate the performance of our proposed MIP framework. We use MATLAB to construct the instances of the data link layer model parameters presented in Section III-B. General Algebraic Modeling System (GAMS) is employed for the solutions of the MIP framework presented in Section III-C. GAMS consists of high-performance solvers for solving MIP models efficiently each of which improves upon the basic approach in different ways to attain an increased solution performance. Hence, when we solve our MIP model using GAMS, CPLEX solver is used to obtain the best solution. The solutions of MIP models utilize algorithms such as branch-and-bound, branch-and-cut, etc. At each step of such algorithms, first the problem without the integrality restrictions on variables (*i.e.*, the Linear Programming relaxation) is solved. Then, if an integer variable (*e.g.*, the one which is actually required to be 0 or 1 in the original problem) has a fractional value in the current solution, then the problem is divided into two subproblems by setting that variable's value to 0 and 1, respectively. Then the new problems are solved recursively in the same manner until the optimal solution is found. This basic method can be improved and solution times can be reduced by incorporating problem specific information in the subproblem creation step. Specific implementation details are beyond the scope of this study.

A. Transitional Region Analysis

We begin our analysis by investigating the transitional regions for the channel model proposed in Section III-B. In a typical wireless link, there are 3 regions, commonly referred to as *connected*, *transitional*, and *disconnected* [33]. The connected region is where the perfect packet reception takes place. The disconnected region occurs when packet reception rate degenerates down to zero. In between the two lies the transitional region [33].

To investigate the transitional region, we present Fig. 3 where we consider a single node pair separated by a distance of d_{int}, and calculate the successful handshake probability, as presented in (11), for various d_{int} values. All data points presented in this Fig. 3 are the averages of 2000 random runs (*i.e.*, at each run path loss values of all links are regenerated). We consider 3 different packet sizes (M_D = 256, 136, and 46 Bytes). ACK packet size is set to 20 Bytes (M_A = 20 Bytes). We utilize 3 different transmission power levels out of 26 available power levels which are denoted as l = 12, l = 19, and l = 26. For the given power levels, we present 3 transitional regions denoted as TR_1, TR_2, and TR_3. The average successful handshake probability keeps a level around 1 (*i.e.*, 100%) until the transitional region where it decreases fairly rapidly to 0. Finally, we observe that effects of packet size on the successful handshake probability is insignificant when compared to d_{int} or transmission power level. In other words, as shown in Fig. 3, the three leftmost data points correspond to the power level of 12 for M_D = 256, 136, and 46 Bytes. It is clear that the data packet size does not have any dominant statistical effect on the average successful handshake probability, or $E[p^{HS,s}]$. The same observation clearly visible for the power levels of 19 and 26 in Fig. 3. At higher power levels (*e.g.*, l = 19 and l = 26), transitional region tends to be wider compared with lower power levels (*i.e.*, l = 12).

For the further analysis in the following subsections, we mark several points on Fig. 3 which are detailed in Table III. We define Y for the power level l = 12; likewise Z for l = 19, and T for l = 26, respectively. Subscripts 0 to 4 in each point represents average successful handshake probability values ($E[p^{HS,s}]$ = 0.999, 0.900, 0.500, 0.100, and 0.001, respectively). Points where $E[p^{HS,s}] = 0.999$ and $E[p^{HS,s}] = 0.001$ are considered as the closest points where the transitional region is about to start and end, respectively.

B. Analysis on Grid Topology

In this subsection, building upon the work from subsection IV-A, we extend our analysis for a grid topology where the base station is placed at the center of a grid area. The distance between adjacent nodes are d_{int} meters chosen from Table III. The number of nodes (N_S) are set to 49, 81, and 121 such that an evenly distributed grid topology can be realized as depicted in Fig. 4. In this subsection and subsection IV-C, (15) is not utilized to determine the transmission power levels, instead, all links use the same predetermined power level l, however, in subsection IV-D, (15) is employed to determine the transmission power levels.

In Fig. 5, we present normalized lifetime values with respect to various payload values for 3 power levels provided in Section IV-A. Note that in the remainder of this work, we present payload values (given in x-axis) in descending order (*i.e.*, 240, 120, 80, 60, 48, 40, and 30 Bytes) since we are interested in the number of generated data packets in each round (s_i) which are in the ascending order (*i.e.*, 1, 2, 3, 4, 5, 6, and 8). For example, when payload value is 240 there is one packet to carry it, for payload of 120, two packets, for 80, 3 packets, *etc*. All values in Fig. 5 are normalized with respect to highest obtained lifetime value. All data points presented in this figure are the averages of 100 random path loss values for all links.

Network lifetime decreases as the payload size decreases for all settings (*e.g.*, for $d_{int} = Y_0$, N_S = 49, l = 12, lifetime decreases 53% when data packet size is decreased from 256 Bytes to 46 Bytes). Normalized network lifetime is maximized for the largest payload size (*i.e.*, M_D = 256 Bytes) regardless of the chosen power level (l). The reason for such behavior is that the effects of higher payload to overhead ratio is dominant over the retransmission effects provided that the operating region is close to the *connected* region. We do not present network lifetime results for links with $E[p^{HS,s}] < 0.900$ because the receiver sensitivity prevents the links with lower received powers to be utilized. Hence, we are left with links with $E[p^{HS,s}] \geq 0.900$ when the receiver sensitivity is in effect. Since the receiver sensitivity prevents us from venturing deep into the transitional region in the following subsection we will not consider the effects of the receiver sensitivity which will enable us to characterize the effects of ignoring a fundamental limit in transceiver technology. Note

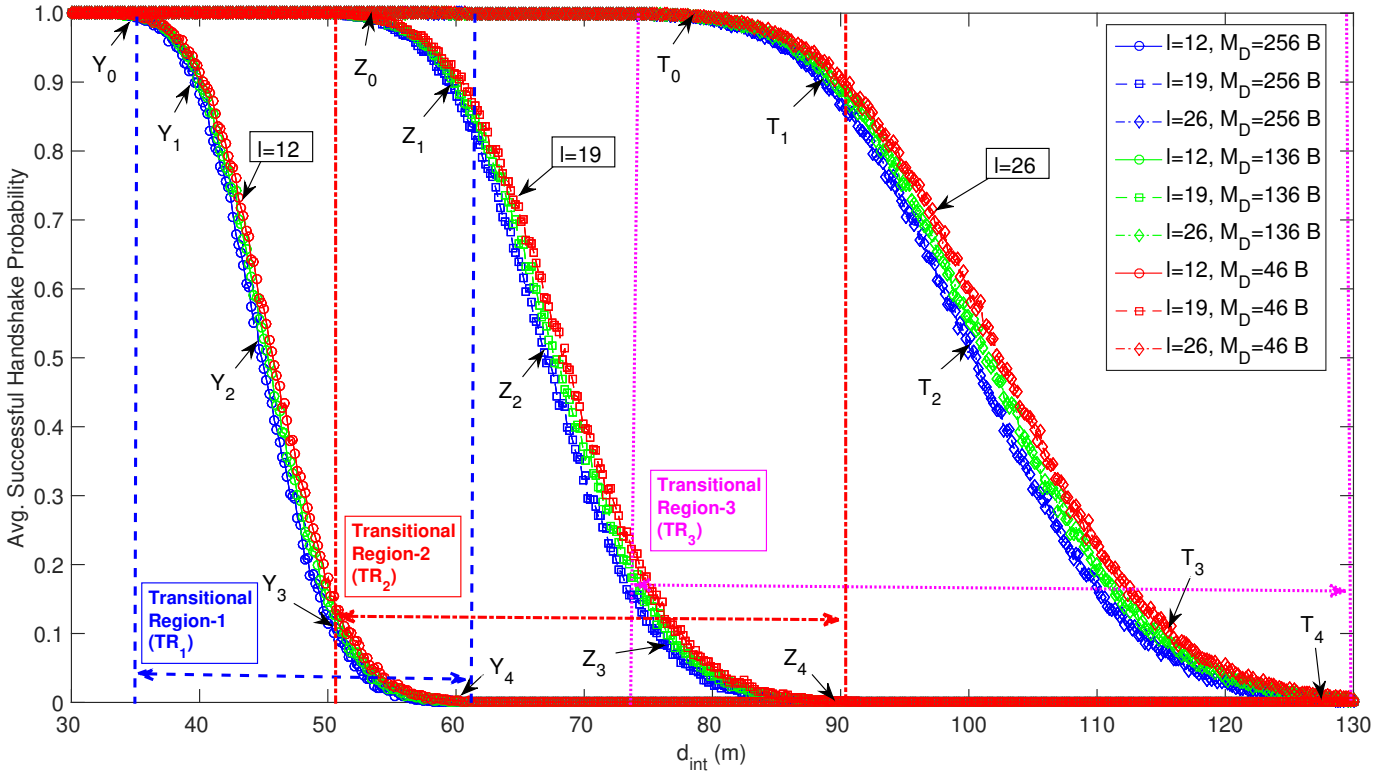

Fig. 3: Inter-node distance (d_{int}) vs. avg. successful handshake probability $E[p^{HS,s}]$ for 3 power levels, packet sizes, and corresponding transitional regions (TR_k).

TABLE III: Measurement points, related d_{int}, and avg. successful handshake probability values ($E[p^{HS,s}]$).

$l = 12$ (TR_1)			$l = 19$ (TR_2)			$l = 26$ (TR_3)		
Parameter	Value	$E[p^{HS,s}]$	Parameter	Value	$E[p^{HS,s}]$	Parameter	Value	$E[p^{HS,s}]$
Y_0	32.01 m	0.999	Z_0	48.09 m	0.999	T_0	70.70 m	0.999
Y_1	39.55 m	0.900	Z_1	59.15 m	0.900	T_1	87.79 m	0.900
Y_2	45.08 m	0.500	Z_2	67.19 m	0.500	T_2	100.4 m	0.500
Y_3	50.60 m	0.100	Z_3	75.73 m	0.100	T_3	111.4 m	0.100
Y_4	58.64 m	0.001	Z_4	88.29 m	0.001	T_4	129.0 m	0.001

that we employed the sensitivity level given in the Mica2 datasheet [30] which is $P_{sns} = -102$ dBm to obtain the results is this subsection. However, if the sensitivity level were to be $P_{sns} \leq -109$ dBm then most of the transitional region would be included the operating region of the Mica2 motes. Hence, in subsection IV-C, we will explore the effects of lower sensitivity threshold on data packet size optimization.

C. Impact of Sensitivity Criterion

Fig. 6 presents the normalized lifetime values with respect to various payload size values. In each subfigure, three pre-determined power levels (*i.e.*, $l = 12$, $l = 19$, and $l = 26$) are employed at network level. d_{int} values are taken for each chosen power level such that $E[p^{HS,s}] = 0.500$ and $E[p^{HS,s}] = 0.900$. For d_{int} values where $E[p^{HS,s}] < 0.500$, network is disconnected thus, we have a network lifetime of 0. When we consider $d_{int} = Y_1$ (or Z_1 or T_1) meters, normalized lifetime decreases down to around 0.54 as the packet size decreases (Fig. 6a–Fig. 6c). Since $E[p^{HS,s}] = 0.900$, links again utilize the highest possible packet size values as the packet errors are almost zero, hence, maximizing the network lifetime.

As we step into the transitional region by increasing d_{int} to Y_2 meters (or Z_2 / T_2 meters where $E[p^{HS,s}] = 0.500$), the trade-off between packet size and network lifetime is revealed clearly (Fig. 6d–Fig. 6f) regardless of the power level that is used at the network level. We observe that maximum payload sizes do not yield maximum lifetimes. Moreover, for $N_S = 121$ and $l = 12$ (or $l = 19$), we have a 0 normalized lifetime when $M_P = 240$ Bytes. Since the channel condition becomes harsher, smaller payload sizes yield maximum lifetimes. For example, for $N_S = 49$ maximum lifetime is obtained when payload size is chosen as 40 Bytes so that the total packet size will be 56 Bytes. As N_S increases, larger payload sizes are chosen to maximize the network lifetime. For example, when $N_S = 81$, 48 Bytes of payload yields the maximum lifetime while for $N_S = 121$, 60 Bytes of payload yields the maximum lifetime.

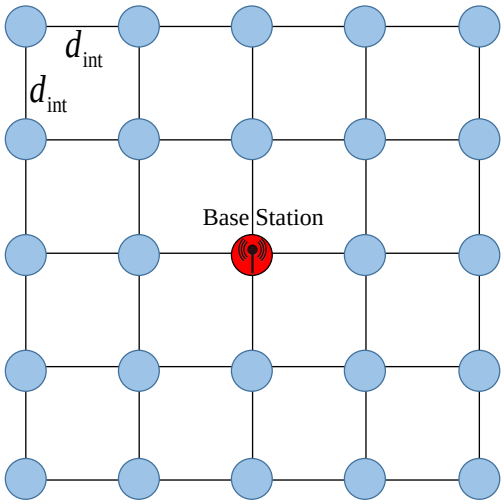

Fig. 4: A grid topology deployment.

When receiver sensitivity is allowed take values that enables the transceivers to operate in the *transitional* region (*i.e.*, $P_{sns} < -102$ dBm), the optimal packet size is different from the maximum packet size provided that the operating region is moved deep into the *transitional* region. Furthermore, under such conditions the trade-off between packet size and network lifetime can clearly be observed. However, the freedom to venture deep into the *transitional* region is very much dependent on the transceiver design, in general, and on the actual receiver sensitivity level of the WSN transceiver, in particular. For example, Mica2 motes which, arguably, are the most widely utilized platforms in experimental WSN research, prevent the nodes to venture deep into the *transitional* region.

D. Analysis on Random Networks

Random node deployment over a two dimensional sensing area is a frequently employed scenario in WSNs. Hence, in this subsection, we consider a random network topology where we use a disk shaped network consisting of N_S sensor nodes and a base station which are uniformly placed within the disk with radius R_{net} and a base station at the center. N_S values are chosen as 60, 90, and 120 nodes. R_{net} is set to 400, 700, and 1000 meters. Note that, in this subsection, we activate the sensitivity criterion back again as in Section IV-B with $P_{sns} = -102$ dBm. The results are averaged over 100 independent runs (*i.e.*, 100 randomly generated topologies). Normalization is achieved by dividing the lifetime values with the maximum lifetime obtained for the same parameter set. Finally, optimal power levels are determined by using the link scope optimization scheme presented in (15).

In Fig. 7, we present normalized lifetime values with respect to the packet size for three N_S values at each subgraph. Furthermore, in each subgraph lifetime values for three network areas are plotted. In Fig. 8, normalized lifetime values are presented for three network area values as functions of packet size at each subfigure and each subfigure contains three lifetime plots for different N_S values. In all settings network lifetime is the highest for the maximum data packet size. The reason for such behavior is that overwhelming majority of the links carrying data have average successful handshake probabilities greater than 0.999 (*i.e.*, $E[p^{HS,s}] \geq 0.999$). Since $E[p^{HS,s}] \geq 0.999$, links utilize the highest possible packet size values as the packet errors are negligible, hence, maximizing the network lifetime.

WSN nodes equipped with batteries have limited lifetime (*i.e.*, when the battery energy is depleted the node is left non-operational). Energy harvesting is an emerging technique and the main idea behind energy harvesting is capturing the energy radiation due to ambient physical phenomena by sensor nodes [34]. Energy acquired by the energy harvesting subsystem is stored and used for data acquisition, signal processing and communications operations [35]. Hence, the capability of energy harvesting is invaluable for prolonging WSN lifetime. Optimizing packet size in conjunction to energy harvesting will lead to further prolonging of the WSN lifetime, hence, packet size optimization and energy harvesting are complementary capabilities in WSNs.

V. Conclusion

In this study, we characterize the impact of joint transmission power level and data packet size optimization on WSN lifetime. We built a novel MIP framework for modeling the optimization problem which sits on top of a realistic link layer abstraction. The link layer abstraction is based on an empirically verified channel model designed specifically for WSNs and the energy model is based on Mica2 motes' energy dissipation characteristics. The main conclusion of this study is that there exists an optimal data packet size for each specific scenario where the network lifetime is higher than other packet sizes. However, this result is observed only if the receiver sensitivity level is low enough to allow the transceivers to be able to operate, in a significant portion of the *transitional* region. When the receiver sensitivity is not low enough, transceivers cannot venture deep into the *transitional* region like transceivers of Mica2 motes. In this case, we show that the maximum network lifetime is achieved for the maximum packet size.

References

[1] M. Erol-Kantarci and H. Mouftah, "Wireless sensor networks for cost-efficient residential energy management in the smart grid," *IEEE Transactions on Smart Grid*, vol. 2, pp. 314–325, 2011.

[2] A. Seema and M. Reisslein, "Towards efficient wireless video sensor networks: A survey of existing node architectures and proposal for a Flexi-WVSNP design," *IEEE Communications Surveys Tutorials*, vol. 13, pp. 462–486, 2011.

[3] J. Barcelo-Ordinas, J. Chanet, K.-M. Hou, and J. Garcia-Vidal, "A survey of wireless sensor technologies applied to precision agriculture," in *Precision agriculture'13*, J. V. Stafford, Ed. Wageningen Academic Publishers, 2013, pp. 801–808.

[4] Z. Cheng, M. Perillo, and W. Heinzelman, "General network lifetime and cost models for evaluating sensor network deployment strategies," *IEEE Transactions on Mobile Computing*, vol. 7, pp. 484–497, 2008.

[5] K. Akkaya and M. Younis, "A survey on routing protocols for wireless sensor networks," *Ad Hoc Networks*, vol. 3, pp. 325–349, 2005.

[6] W. Dong, X. Liu, C. Chen, Y. He, G.Chen, Y. Liu, and J. Bu, "DPLC: dynamic packet length control in wireless sensor networks," in *Proceedings of the IEEE International Conference on Computer Communications (INFOCOM)*, 2010, pp. 1–9.

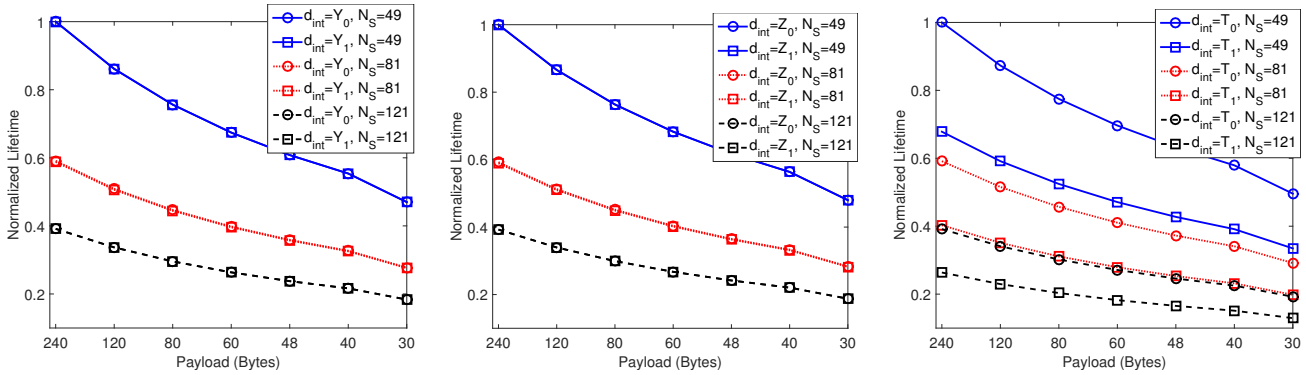

(a) $l = 12$ (b) $l = 19$ (c) $l = 26$

Fig. 5: Normalized lifetimes wrt payload size for various power levels (l) and number of nodes (N_S) for the grid topology.

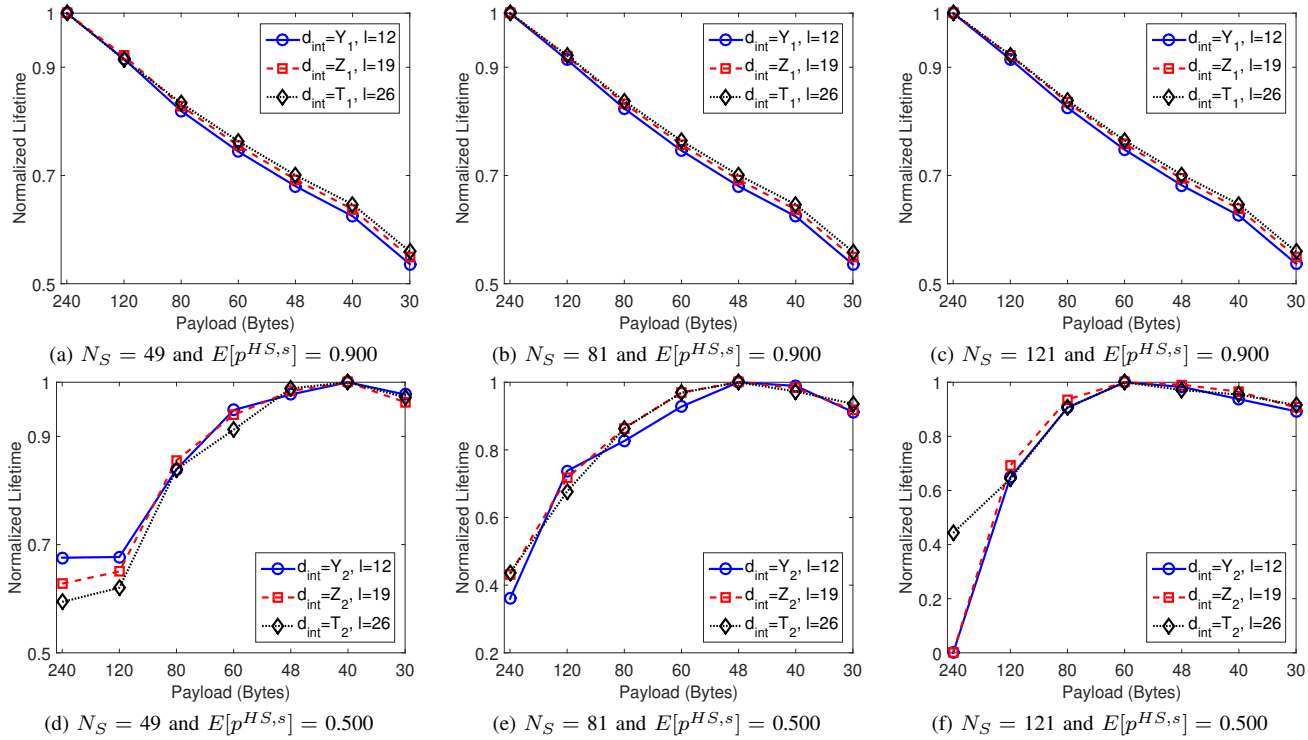

(a) $N_S = 49$ and $E[p^{HS,s}] = 0.900$ (b) $N_S = 81$ and $E[p^{HS,s}] = 0.900$ (c) $N_S = 121$ and $E[p^{HS,s}] = 0.900$

(d) $N_S = 49$ and $E[p^{HS,s}] = 0.500$ (e) $N_S = 81$ and $E[p^{HS,s}] = 0.500$ (f) $N_S = 121$ and $E[p^{HS,s}] = 0.500$

Fig. 6: Normalized lifetimes wrt payload size for various power levels (l) and number of nodes (N_S) for the grid topology without the sensitivity criterion.

[7] M. Holland, T. Wang, B. Tavli, A. Seyedi, and W. Heinzelman, "Optimizing physical-layer parameters for wireless sensor networks," *ACM Transactions on Sensor Networks*, vol. 7, no. 4, pp. 28:1–28:20, 2011.

[8] A. Nandi, D. Bepari, and S. Kundu, "Optimal transmit power and packet size in wireless sensor networks in shadowed channel," *ACEEE International Journal on Communication*, vol. 1, no. 2, pp. 39–44, 2010.

[9] A. Nandi and S. Kundu, "On energy level performance of adaptive power based WSN in shadowed channel," in *Proceedings of the International Conference on Devices and Communications (ICDeCom)*, 2011, pp. 1–5.

[10] S. Basagni, C. Petrioli, R. Petroccia, and M. Stojanovic, "Optimized packet size selection in underwater wireless sensor network communications," *IEEE Journal of Oceanic Engineering*, vol. 37, no. 3, pp. 321–337, 2012.

[11] L. Jung and A. Abdullah, "Underwater wireless network energy efficiency and optimal data packet size," in *Proceedings of the International Conference on Electrical, Control and Computer Engineering (INECCE)*, 2011, pp. 178–182.

[12] M. Vuran and I. Akyildiz, "Cross-layer packet size optimization for wireless terrestrial, underwater, and underground sensor networks," in *Proceedings of the Conference on Computer Communications*, 2009, pp. 13–18.

[13] Y. Li, X. Qi, Z. Ren, G. Zhou, D. Xiao, and S. Deng, "Energy modeling and optimization through joint packet size analysis of BSN and Wi-Fi networks," *IEEE Transactions on Parallel and Distributed Systems*, vol. 24, pp. 1741–1751, 2013.

[14] M. Mohammadi, Q. Zhang, E. Dutkiewicz, and X. Huang, "Optimal frame length to maximize energy efficiency in IEEE 802.15.6 UWB body area networks," *IEEE Wireless Communications Letters*, vol. 3, no. 4, pp. 397–400, 2014.

[15] K. Lendvai, A. Milankovich, S. Imre, and S. Szabo, "Optimized packet size for energy efficient delay tolerant sensor networks," in *Proceedings of the IEEE International Conference on Wireless and Mobile Computing, Networking and Communications (WiMob)*, 2012, pp. 19–25.

[16] U. Datta and S. Kundu, "Packet size optimization for multi hop CDMA wireless sensor networks with nearest neighbors based routing," in *Proceedings of the International Conference on Emerging Applications*

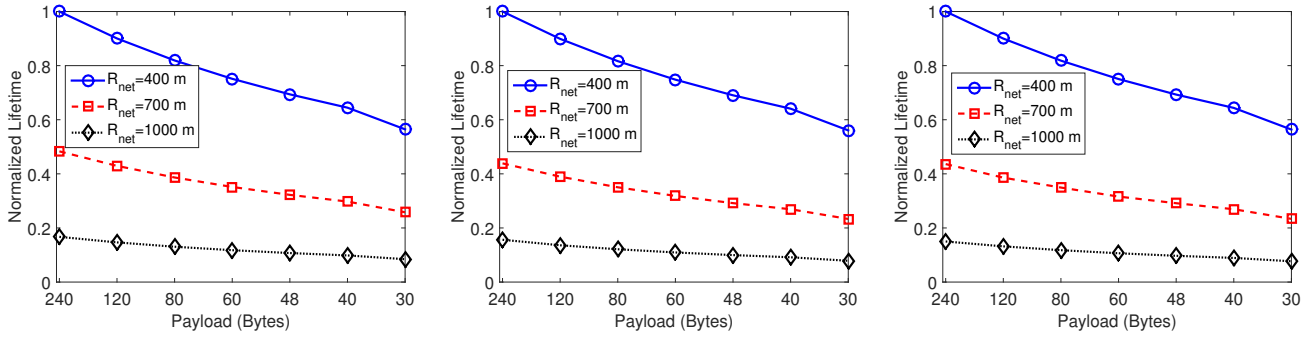

(a) $N_S = 60$ (b) $N_S = 90$ (c) $N_S = 120$

Fig. 7: Normalized lifetimes wrt. packet size for various N_S values when R_{net} = 400, 700 and 1000 m for the random network.

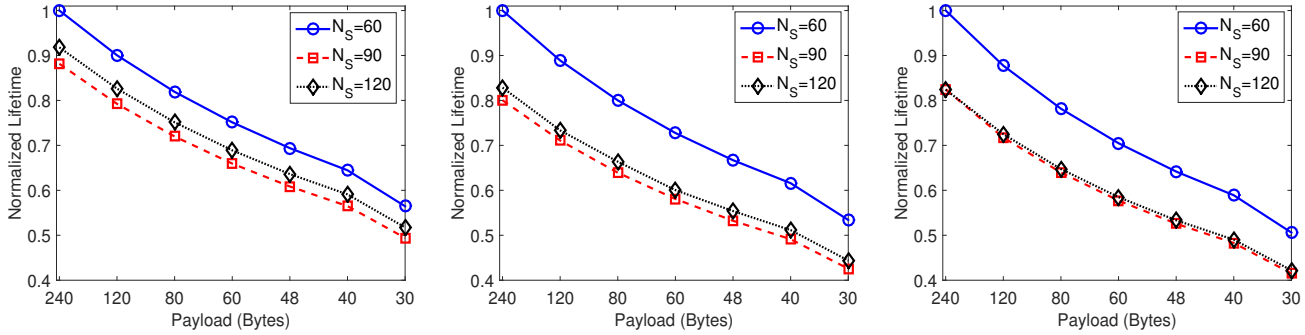

(a) R_{net} = 400 m (b) R_{net} = 700 m (c) R_{net} = 1000 m

Fig. 8: Normalized lifetimes wrt. packet size for various R_{net} values when N_S = 60, 90, and 120 for the random network.

of Information Technology (EAIT), 2012, pp. 408–412.

[17] C. Noda, S. Prabhi, and M. Alves, "On packet size and error correction optimisations in low-power wireless networks," in *Proceedings of the IEEE International Conference on Sensing, Communication and Networking (SECON)*, 2013, pp. 212–220.

[18] U. Datta, C. Kundu, and S. Kundu, "Performance of an optimum packet based cdma wireless sensor networks in presence of correlated interferers," in *Proceedings of the IEEE International Conference on Computer & Communication (ICCCT)*, 2010, pp. 23–27.

[19] T. Zhao, T. Guo, and W. Yang, "Optimal transmission radii and packet size for wireless sensor networks based on bi-ievel programming model," in *Proceedings of the International Conference on Intelligent Computing and Integrated Systems (ICISS)*, 2010, pp. 840–844.

[20] M. Oto and O. Akan, "Energy-efficient packet size optimization for cognitive radio sensor networks," *IEEE Transactions on Wireless Communications*, vol. 11, no. 4, pp. 1544–1553, 2012.

[21] S. Abdulhadi, M. Naeem, M. Jaseemuddin, and A. Anpalagan, "Optimized packet size for energy efficient cooperative wireless ad-hoc networks," in *Proceedings of the IEEE International Conference on Communications Workshops (ICC)*, 2013, pp. 581–585.

[22] Y. Sankarasubramaniam, I. Akyildiz, and S. McLaughlin, "Energy efficiency based packet size optimization in wireless sensor networks," in *Proceedings of the IEEE International Workshop on Sensor Network Protocols and Applications*, 2003, pp. 1–8.

[23] K. Lendvai, A. Milankovich, S. Imre, and S. Szabo, "Optimized packet size for energy efficient delay- tolerant sensor networks with FEC," in *Proceedings of the International Conference on Telecommunications (ConTEL)*, 2013, pp. 87–94.

[24] N. Xia, R. Feng, and L. Xu, "SPSA based packet size optimization algorithm in wireless sensor networks," in *Proceedings of the International Conference on Wireless Algorithms, Systems, and Applications (WASA)*, 2012, pp. 1112–1119.

[25] S. Ci, H. Sharif, and K. Nuli, "Study of an adaptive frame size predictor to enhance energy conservation in wireless sensor networks," *IEEE Journal on Selected Areas in Communications*, vol. 23, pp. 283–292, 2005.

[26] A. Akbas, H. Yildiz, and B. Tavli, "Data packet length optimization for wireless sensor network lifetime maximization," in *Proceedings of the International Conference on Communications (COMM)*, 2014, pp. 321–326.

[27] B. Sundararaman, U. Buy, and A. Kshemkalyani, "Clock synchronization for wireless sensor networks: A survey," *Ad Hoc Networks*, vol. 3, pp. 281–323, 2005.

[28] S. Ganeriwal, R. Kumar, and M. B. Srivastava, "Timing-sync protocol for sensor networks," in *Proceedings of the ACM Conference on Embedded Networked Sensor Systems (SenSys)*, 2003, pp. 138–149.

[29] K. Bilinska, M. Filo, and R. Krystowski. (2007) Mica, Mica2, MicaZ. [Online]. Available: http://wwwpub.zih.tu-dresden.de/ dargie/wsn/slides/students/MICA.ppt

[30] J. Vales-Alonso, E. Egea-Lopez, A. Martinez-Sala, P. Pavon-Marino, M. V. Bueno-Delgado, and J. Garcia-Haro, "Performance evaluation of MAC transmission power control in wireless sensor networks," *Computer Networks*, vol. 51, pp. 1483–1498, 2007.

[31] H. U. Yildiz, B. Tavli, and H. Yanikomeroglu, "Transmission power control for link level handshaking in wireless sensor networks," *IEEE Sensors Journal*, vol. 16, pp. 561–576, 2016.

[32] A. S. Martinez-Sala, J. M. M. G. Pardo, E. Egea-Lopez, J. Vales-Alonso, L. Juan-Llacer, and J. Garcia-Haro, "An accurate radio channel model for wireless sensor networks simulation," *Journal of Communications and Networks*, vol. 7, no. 4, pp. 401–407, 2005.

[33] M. Zuniga and B. Krishnamachari, "Analyzing the transitional region in low power wireless links," in *Proceedings of the IEEE International Conference on Sensing, Communication and Networks (SECON)*, 2004, pp. 517–526.

[34] Z. Wan, Y. Tan, and C. Yuen, "Review on energy harvesting and energy management for sustainable wireless sensor networks," in *Proceedings of the IEEE International Conference on Communication Technology (ICCT)*, 2011, pp. 362–367.

[35] C. Alippi and C. Galperti, "An adaptive system for optimal solar energy harvesting in wireless sensor network nodes," *IEEE Transactions on Circuits and Systems I: Regular Papers*, vol. 55, pp. 1742–1750, 2008.

Ayhan Akbas received the B.Sc. and M.Sc. degrees in electrical and electronics engineering from the Middle East Technical University, Ankara, Turkey in 1991 and 1995, respectively. He is currently pursuing the Ph.D. degree in computer engineering at TOBB University of Economics and Technology, Ankara, Turkey. He worked for Siemens, Sun Microsystems, and NEC at technical and management positions on the industrial and military projects. He is currently the founder and CEO of Modula Inc. which specializes on embedded system design. His areas of interest include embedded system design, wireless sensor networks, mobile networks, IoT, and optimization.

Huseyin Ugur Yildiz received the BS degree from the department of electrical and electronics engineering, Bilkent University, Ankara, Turkey, in 2009, MS and PhD degrees from TOBB University of Economics and Technology, Ankara, Turkey, in 2013, and 2016, respectively. He is with Turkish Aerospace Industries (TAI), Ankara, Turkey, as an avionics design engineer focusing on the design of network & communications architecture of the ANKA unmanned aerial vehicle project. Prior to joining TAI, he worked as a network engineer at Turk Telekom, Ankara, Turkey, for 5 years. His research focuses on to apply optimization techniques to model and analyze research problems addressed for wireless communications, wireless sensor networks, and ad hoc networks. He is a student member of the IEEE.

Bulent Tavli is a professor at the Electrical and Electronics Engineering Department, TOBB University of Economics and Technology, Ankara, Turkey. He received the BSc degree in Electrical & Electronics Engineering in 1996 from the Middle East Technical University, Ankara, Turkey. He received the MSc and PhD degrees in Electrical and Computer Engineering in 2001 and 2005 from the University of Rochester, Rochester, NY, USA. Optimization, mathematical programming, wireless communications, computer networks, embedded systems, digital circuit design, information security, forensics, smart grid, software defined networks, and human-machine systems are his current research areas.

Suleyman Uludag is an Associate Professor of Computer Science at the University of Michigan - Flint. His research interests have been around secure data collection, Smart Grid communications, Smart Grid privacy, Smart Grid optimization, demand response bidding privacy, Denial-of-Service in the Smart Grid, cybersecurity education and curriculum development, routing and channel assignment in Wireless Mesh Networks, Quality-of-Service (QoS) routing in wired and wireless networks, topology aggregation.